

Simulation of Residual Deformation from a Forming and Welding Process using LS-DYNA[®]

Mikael Schill¹, Eva-Lis Odenberger²

¹DYNAmore Nordic AB, Sweden

²Industrial Development Centre in Olofström AB, Sweden

Abstract

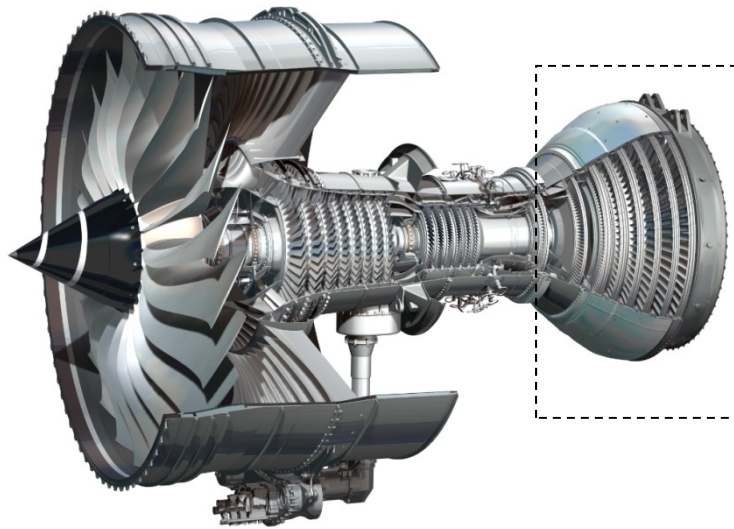
*Predicting the finished geometry of a part is a major issue for the manufacturing industry. This is a complex task, especially if the manufacturing involves several types of processes. In order to succeed, the complete manufacturing process has to be included in the simulation. For sheet metal forming, this has been done for quite some time where trimming, forming and springback are simulated in consecutive order. However, there are other manufacturing processes which affect the geometry of the finished part. In this paper, a welding process is added to the manufacturing process chain. The welding simulation is done using the novel material model *MAT_CWM with ghost element functionality.*

The aim of the paper is to investigate how the different process stages affect the final geometry of the part and how this is efficiently and accurately simulated with LS-DYNA. Further, an attempt is made to improve the part tolerance by springback compensation of the forming tools accounting for deviance from both springback and weld deformation.

Introduction

Traditionally, load carrying structures in aero engines has been built up by large single castings of high temperature materials such as titanium alloys or nickel-based superalloys, see Figure 1. However, the aero engine industry is now moving towards a more fabrication based manufacturing alternative using small ingots, forgings and thin metal sheets which are welded together. The benefits from this are several. Firstly, the manufacturer can rely on more suppliers to produce parts which will reduce the cost. Also, the manufacturing of sheet metal parts is much cheaper compared to casting of large components. Secondly, this alternative provides a more lightweight approach where the thickness and material of each part can be chosen more freely compared to a machined alternative.

However, the benefits above do come with a number of challenges. Due to the vast number of parts, the industry needs a tool for reducing the product and manufacturing process design time. Advanced Finite Element (FE) simulations has proven to be such a tool where virtual models are produced of each process step and the user can predict the final part tolerance, properties and risk for failure. In the sheet metal forming community this is used frequently with excellent results, see e.g. Odenberger et al. [1]. However, the manufacturing of these parts includes one or several welding process steps that need to be included in the virtual process chain. The welding process will cause deformation of the part that can force the part out of shape tolerance. Also, the aerospace industry demands extremely high safety and reliability and life time analysis is an important design step. Here, manufacturing analysis can provide useful information concerning the history of the part including e.g. residual stress and heat affected zones, see Tersing et al.[3]. Welding simulation functionality in LS-DYNA has been further improved by the material model *MAT_CWM that has been developed especially for this purpose.



The Trent XWB will power the Airbus A350 XWB

Figure 1: Aero engine with load carrying structure in the back of the engine

Simulation of the manufacturing process chain

The simulation of the manufacturing process of these parts will require a variety of different solvers and element types, see Figure 3. For instance, the forming simulation is preferably done using the explicit solver with shell elements for simulation time reasons. Also, the part is trimmed at the end of the forming stage and this is not possible using solid elements. On the other hand, the welding simulations are preferably performed using solid elements and the implicit solver. It will also require a thermo-mechanical coupling to account for the temperature dependent material properties. The mesh used in the forming simulation will differ substantially from the mesh used in the welding simulations, see Figure 2. Since the different process steps require different types of simulation models it is not possible to do this without mapping between different meshes and mesh types.

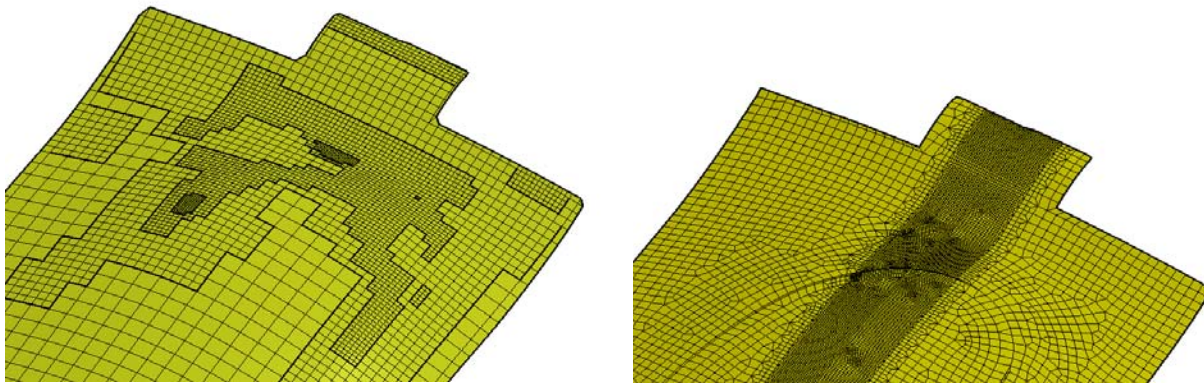


Figure 2: Forming simulation mesh (left) and welding simulation mesh (right)

The process chain starts with a forming simulation, see Figure 3. The sheet metal parts used in the aero engine are typically smoothly double curved parts. The parts are rather formed than

stretched without considerable membrane straining rendering them especially vulnerable for springback deformation. After the forming simulation, the part is trimmed to final part geometry. Before springback simulation, the forming simulation results are mapped to a solid element mesh. The reason for this is that a solid element mesh is needed for the welding simulation and CAD geometry is available of the nominal part and not the springback geometry. The mapping is performed using LS-PrePost[®] v4.2 which is described below. Next, the welding simulation is performed using the novel *MAT_CWM material model. The welding process will introduce additional residual stresses that will further deform the part out of tolerance. In the manufacturing process presented in Figure 3, a springback compensation stage is introduced that will compensate for the deformation by modifying the tool geometry. The design loop will continue until the part is within shape tolerance.

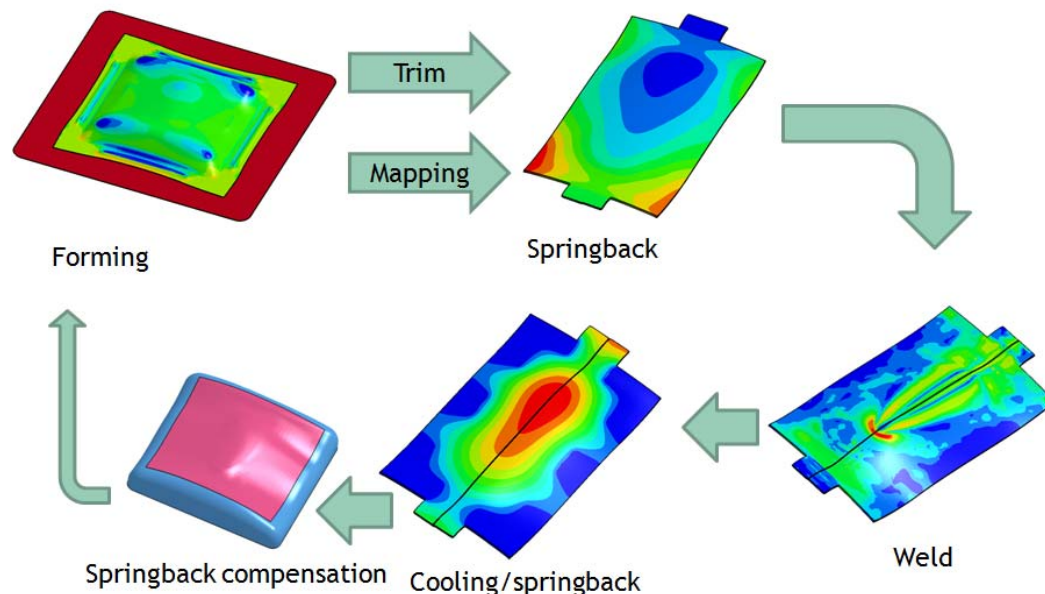


Figure 3: Virtual manufacturing process chain

FE models

The material model used in the welding simulations is the novel *MAT_CWM (*MAT_270) which has been developed especially for welding simulations. The procedure for using this material model has been described by Lindström [4]. Also, it has been verified against benchmark experiments of multi pass girth welds in Lindström et al. [5]. The CWM material model has a number of features that enables welding simulations. Firstly, the elements can be either material or ghost. Ghost material is typically used for the weld filler material that is added to the weld seam. The ghost material is given silent properties which are used until the material is activated. The properties are the Young's modulus, Poisson's ratio, coefficient of thermal expansion, specific heat and heat transfer coefficient. These should be wisely such that the values correspond to "void" and does not affect the solution. On the other hand numerical stability has to be maintained. As the weld heat source heats up the material above the melting point, the material is activated and given properties of the actual base material of that temperature. The activation temperature is input as a temperature interval for numerical reasons where the properties are linearly interpolated through the material activation indicator γ according to

$$\gamma = \min\left(1, \max\left[0, \frac{T_{max} - T_{act}^{start}}{T_{act}^{end} - T_{act}^{start}}\right]\right)$$

where T_{max} is the maximum temperature value of the integration point. Thus, e.g. in the case of Young's modulus, the material is activated through

$$E = E(T)\gamma + E_{GHOST}(1 - \gamma)$$

The mechanical *MAT_CWM has a thermal counterpart with thermal activation and ghost properties denoted *MAT_THERMAL_CWM. Secondly, *MAT_CWM has anneal functionality meaning that above a user-specified temperature, the history variables such as effective plastic strain and/or backstress are zeroed out and the material properties are reset to virgin. This is also done using a temperature interval for numerical reasons. Beyond the annealing temperature, the material will behave as ideal plastic without evolution of the plastic strain or backstress variables. Further, it has linear isotropic/kinematic hardening and it is based on von Mises yield criterion where all material properties are temperature dependent.

The material used in this study is the Inconel 718 nickel-based superalloy. Material data is found in Desphande et al. [6], see Figure 4 and Figure 5.

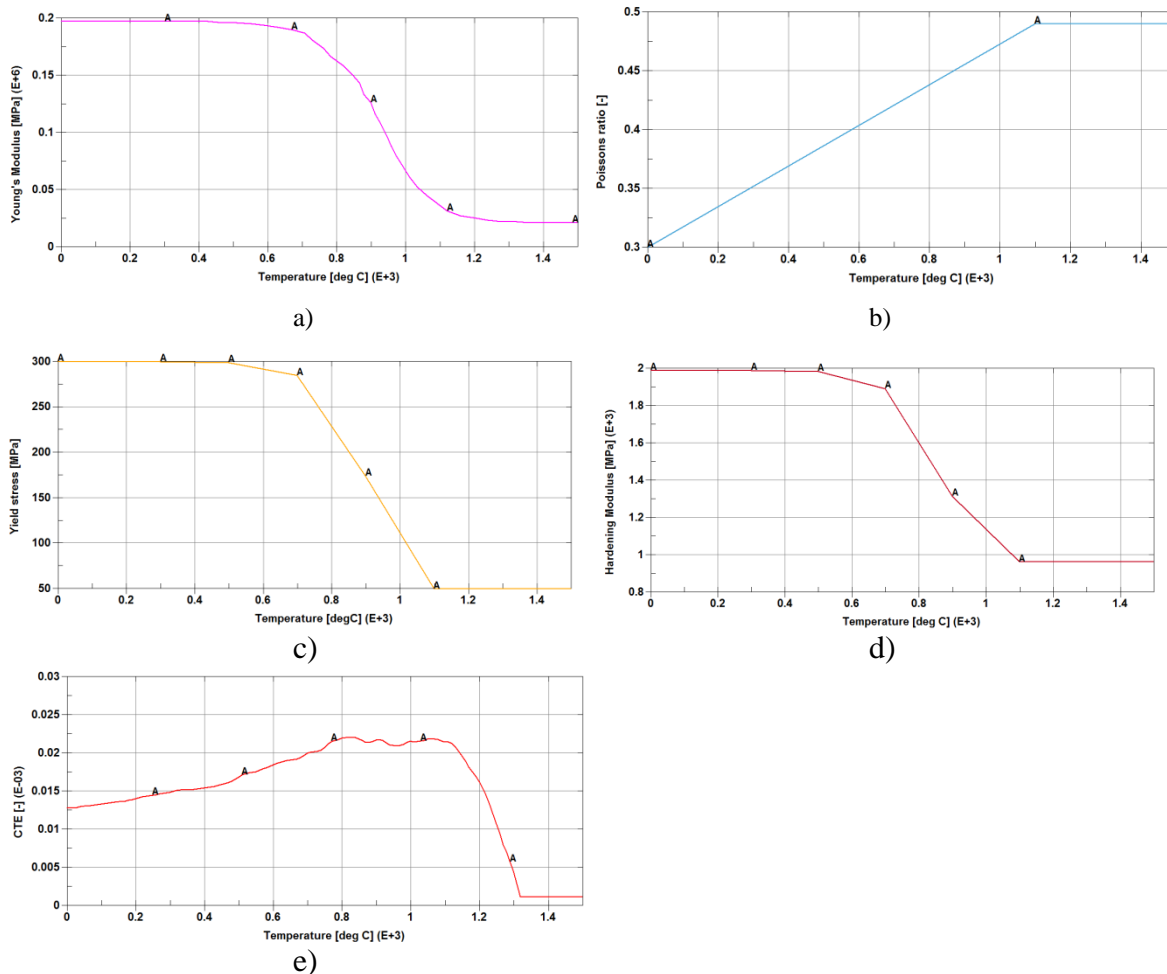


Figure 4: Mechanical material data from Desphande et al. [6], a) Young's Modulus, b) Poisson's ratio, c) Yield stress, d) Hardening modulus and e) Coefficient of thermal expansion

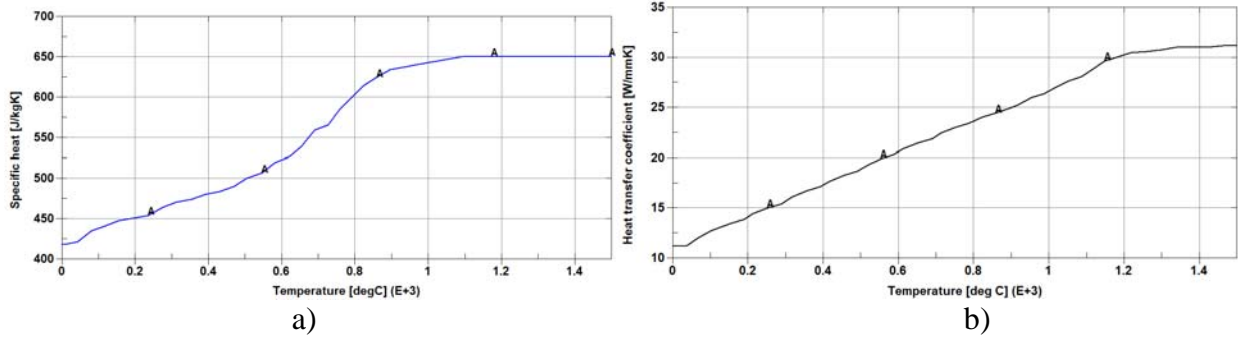


Figure 5: Thermal material data from Desphande et al. [6], a) specific heat and b) heat transfer coefficient.

The ghost properties and corresponding activation and anneal temperatures are found in Table 1.

Table 1: Ghost properties of Inconel 718 used in the study

Young's Modulus [MPa]	2.12e4
Poisson's ratio [-]	0.499
CTE [1/deg]	0.
Specific heat [J/kgK]	650
Heat transfer coefficient [W/mK]	0.01
Anneal temperature [C]	1200-1210
Activation temperature [C]	1250-1350

The forming simulation is done using underintegrated shell elements and adaptivity. The part is then trimmed and mapped to a fully integrated solid element mesh using the novel shell to solid mapping functionality in LS-PrePost v4.2, see Figure 6.

The mapping algorithm is divided into a through thickness and an in-plane part. The through thickness parametric position of the solid element integration point is determined and mapped against its shell counterpart. In the in-plane mapping, the parametric position of the integration point is determined by projecting the integration point on the shell mesh. The corresponding mapped value is then determined by a bi-linear interpolation using the shape functions.

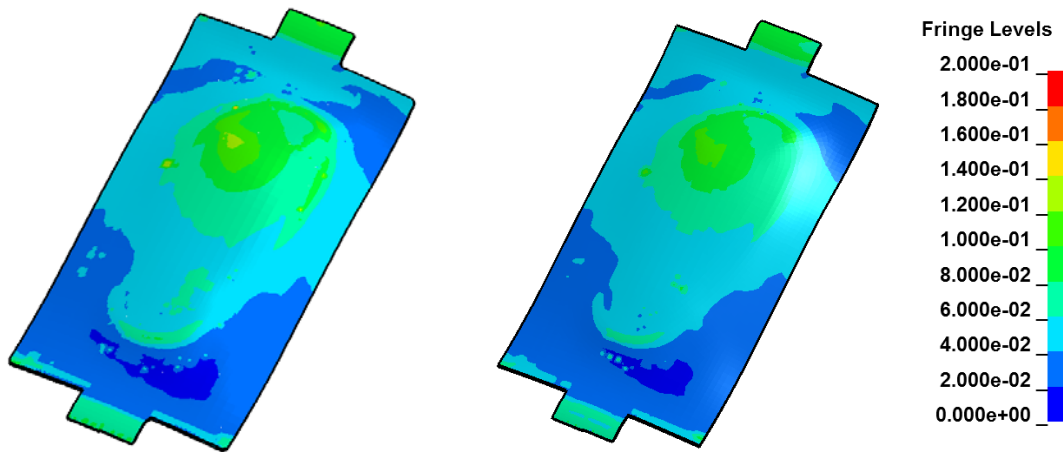


Figure 6: Shell (left) to solid (right) mapping using LS-PrePost.

After springback, the part is cut in the middle and clamped for the welding, see Figure 7. The parts are tack welded before seam welded. The tack welding is not simulated. It is however modeled by assigning parts of the weld seam as bulk material. The weld simulation is done using the implicit solver and a coupled thermo-mechanical solution. A constant thermal and mechanical timestep is used where the weld source moves 2/3 of an element in one timestep.

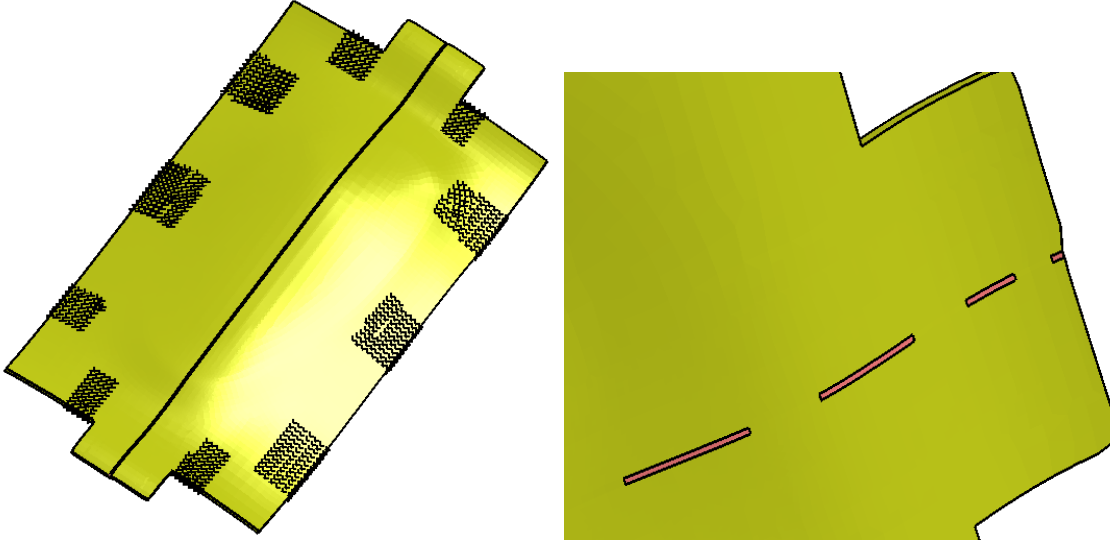


Figure 7: Clamping constraints (left) and ghost elements (pink) and tack welds right.

The heat from the weld torch is applied using the Goldak double ellipsoid heat source, see Goldak et al. [7]. The weld source origin is defined in a node that moves by a prescribed displacement. The heat is applied to the integration points inside the ellipsoid region defined by the weld pool width (b), depth (c), and forward (a_f) and backward (a_r) lengths, see Figure 8.

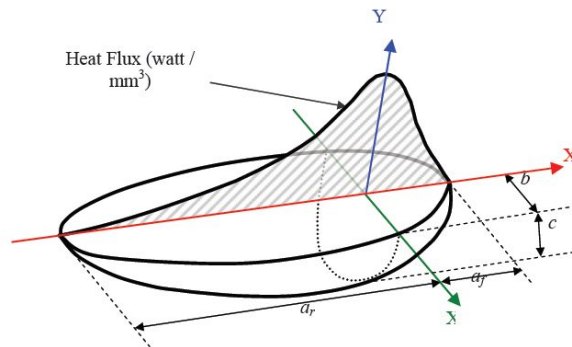


Figure 8: Goldak double ellipsoid heat source

The applied power is 600W and the weld source moves with 3 mm/s. The welded part is then transferred to a cooling simulation using automatic thermal and mechanical timestepping for simulation time efficiency. It is assumed that the part is kept in the welding fixture during cooling. Thus, the last process stage is a springback step where the elastic stresses are released and the final part geometry is received.

Results

During the welding simulation the weld filler elements are activated as they are heated above the melting temperature, see Figure 9. Activated material is set to 1 in history variable 9. The effect of the *MAT_CWM anneal functionality is also visible, where the plastic strain is set to zero wherever the material experience temperatures above the anneal temperature set by the user, see Figure 10. Also, using history variable 10 it is possible to post-process the highest temperature experienced by the element. This is useful when evaluating e.g. the heat affected zone.

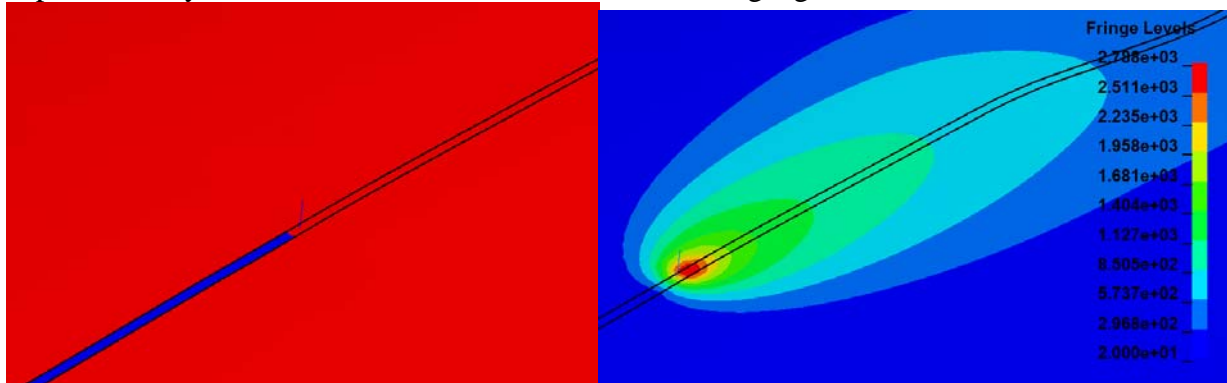


Figure 9: Element activation (red) and welding temperatures.

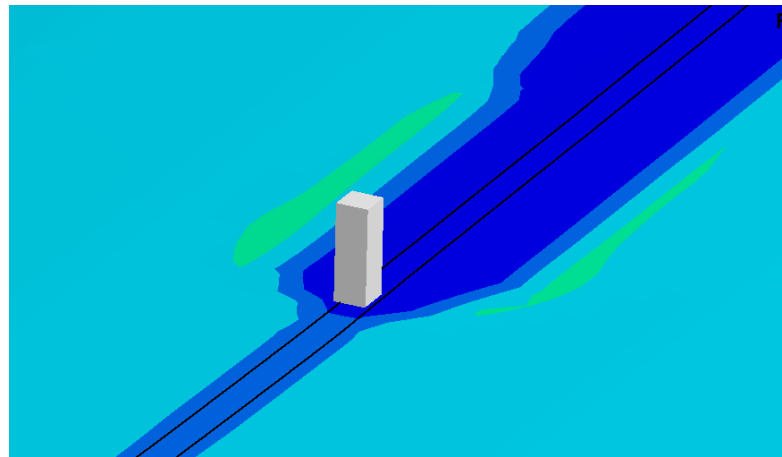


Figure 10: Plastic strain is set to zero above the anneal temperature

The stress state in the part is affected by the heating and cooling of the weld area. Figures 11 through 12 present a typical transverse and longitudinal stress states across the weld after forming, welding and cooling. It is evident that the moderate residual stresses from the forming are severely influenced by the welding. In transverse direction, the stress is in a compressive state, but it is quite smooth over the welded area. However, in the longitudinal direction, the stress has a significant jump over the heat affected zone which is due to the annealing of the material.

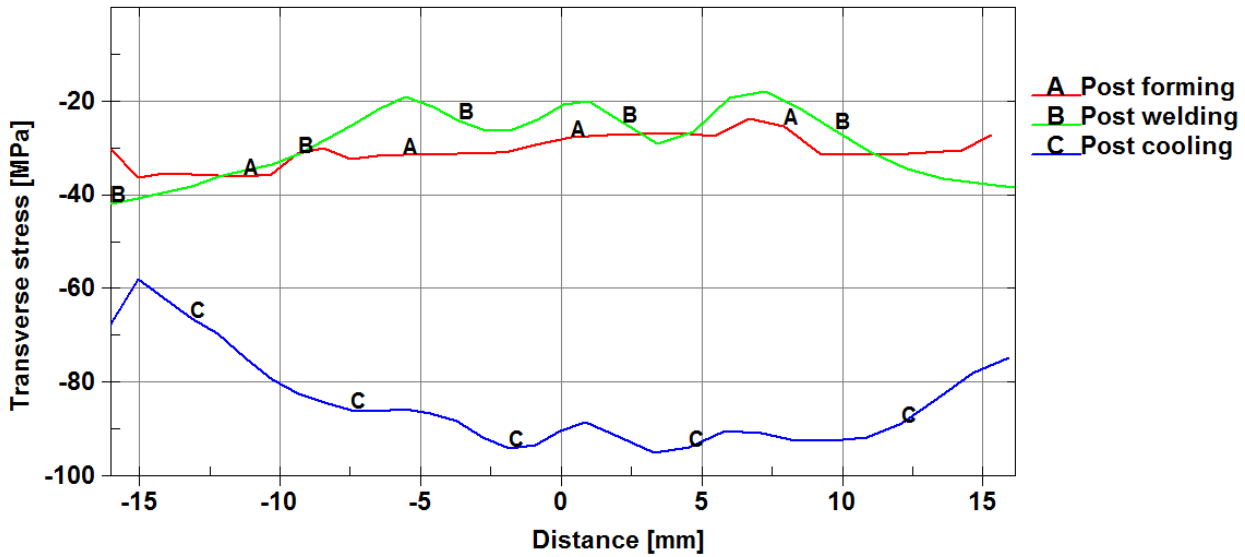


Figure 11: Transverse stress across to the weld after forming, weld and cooling

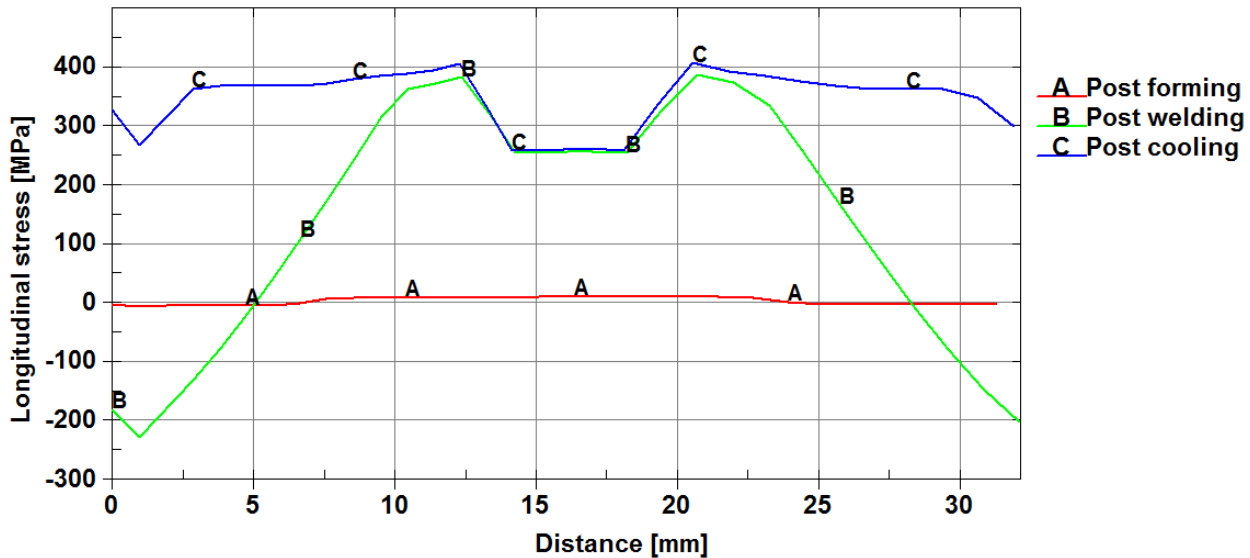


Figure 12: Longitudinal stress across the weld after forming, weld and cooling

The part will be forced out of tolerance by both the elastic springback and the welding stage. Figure 13 presents the shape deviation after forming and welding. It is evident that the part shape changes during welding and in this case, the part is forced further away from the nominal part shape. Several ways exist for trying to limit the part deviation. The part clamping can be modified as well as the welding parameters. In this study, tool shape compensation using *INTERFACE_COMPENSATION_NEW is used. The tools are modified with a scale-factor of 1, and the process chain is simulated once again. The final shape deviation after forming, welding and cooling is presented in Figure 14. By one compensation stage, the maximum deviation is reduced from 3.1 to 0.6 mm and the part tolerance is improved in the complete part. The part tolerance can be improved by further compensation iterations or another choice of compensation scale-factor.

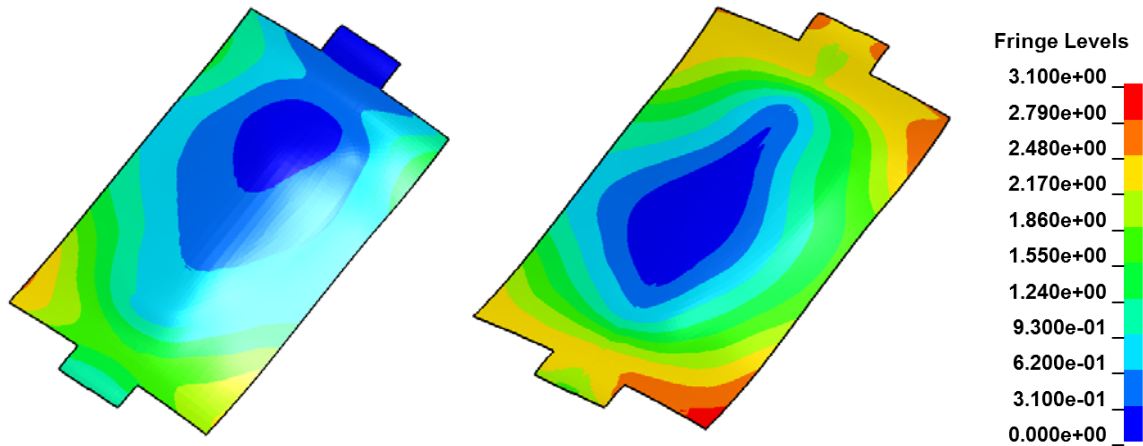


Figure 13: Part deviation after forming (left) and welding (right)

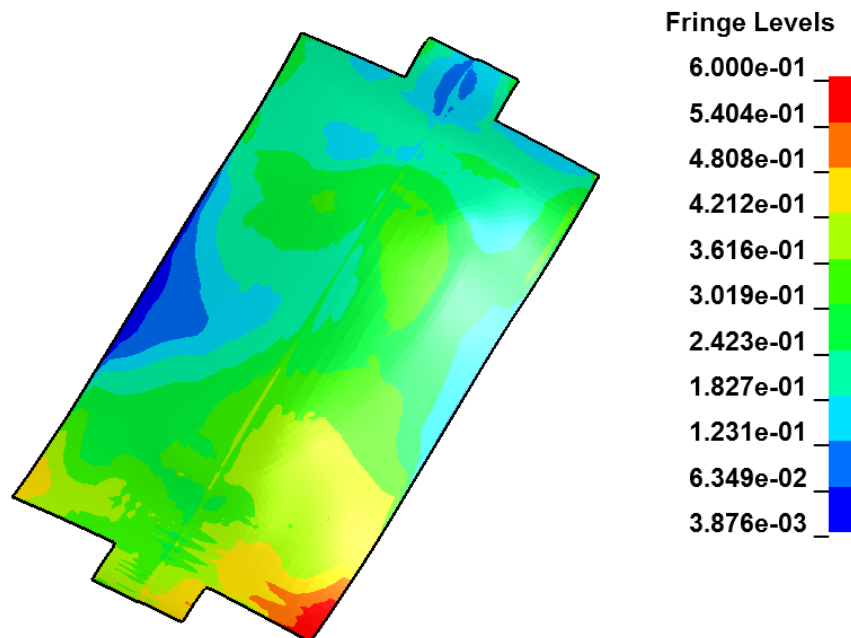


Figure 14: Part deviation after shape compensation

Discussion

In this paper it has been shown that the methodology of compensating the forming tools of these smoothly curved aero engine parts for shape deviation will converge to a part within tolerance. The simulation of the process chain of these parts is complicated by the fact that it contains both forming and welding. To provide for this it is necessary to use different solvers, coupled simulations and element types. The use of one code that supports all the necessary solution schemes is of course a huge benefit in this case. Also, the novel mapping functionality in LS-PrePost will enable the user to use whatever modeling technique necessary for the respective manufacturing stages without worrying of transferring the data to the next process stage.

References

- [1] Odenberger, E-L, Jansson, M., Thilderkvist P., Gustavsson, H., Oldenburg, M., "A short lead time methodology for design, compensation and manufacturing of deep drawing tools for Inconel 718", Proc. Of IDDRG 2008 International Conference, (2008)
- [2] Odenberger, E-L, Schill, M., Oldenburg, M. Thermo-mechanical sheet metal forming of aero engine components in Ti-6Al-4V : Part 2 : Constitutive modelling and validation, International Journal of Material Forming, 6:3 pp 403-416, (2013)
- [3] Tersing, H., Lorentzon, J., Francois, A., Lundbäck, A., Babu, B., Barboza, J., Bäcker, V., Lindgren, L-E., "Simulation of manufacturing chain of a titanium aerospace component with experimental validation", Finite Elements in Analysis and Design, 51, pp 10-21, (2012)
- [4] Lindström, P.R.M, "DNV Platform of Computational Welding Mechanics", Proc. Of Int. Inst. Welding 66th Annual Assembly 6, (2013)
- [5] Lindström, P.R.M, Josefson, L.B., Schill, M., Borrvall, T., " Constitutive Modelling and Finite Element Simulation of Multi Pass Girth Welds", Proc. Of NAFEMS NORDIC Conference, Gothenburg May 22-23, (2012)
- [6] Desphande, A.A., Tanner, D.W.J., Sun, W., Hyde, T.H., McCartney, G., "Combined butt joint welding and post weld heat treatment simulation using SYSWELD and ABAQUS", Proc. Of Inst. Mech. Eng., 225:1 pp 1-10, (2011)
- [7] Goldak, J., Chakravarti, A., Bibby, M., "A Double Ellipsoid Finite Element Model for Welding Heat Sources", IIW Doc.No. 212-603-85, (1985)